Smart Mater. Struct. 5 (1996) 255–260. Printed in the UK

Super-active shape-memory alloy composites

Ron Barrett and R Steven Gross

Aerospace Engineering Department, Auburn University, Auburn, AL 36849-5338, USA

Received 10 July 1995, accepted for publication 11 January 1996

Abstract. A new type of very-low-stiffness super-active composite material is presented. This laminate uses shape-memory alloy (SMA) filaments which are embedded within a low-hardness silicone matrix. The purpose is to develop an active composite in which the local strains within the SMA actuator material will be approximately 1%, while the laminate strains will be at least an order of magnitude larger. This type of laminate will be useful for biomimetic, biomedical, surgical and prosthetic applications in which the very high stiffness and actuation strength of conventional SMA filaments are too great for biological tissues. A modified form of moment and force-balance analysis is used to model the performance of the super-active shape-memory alloy composite (SASMAC). The analytical models are used to predict the performance of a SASMAC pull–pull actuator which uses 10 mil diameter Tinel alloy K actuators embedded in a 0.10" thick, 25 Durometer silicone matrix. The results of testing demonstrate that the laminate is capable of straining up to 10% with theory and experiment in good agreement. Fatigue testing was conducted on the actuator for 1 000 cycles. Because the local strains within the SMA were kept to less than 1%, the element showed no degradation in performance.

1. Introduction

In the past five years, a great deal of progress has been made in the area of artificial muscles and biological tissues. Most of these efforts have been concentrated in the area of polymer research and have yielded a host of new materials which are capable of sizable actuation strains. The work of Shiga and Kurauchi [1] examined deformations which may be generated in polyelectrolyte gels which are exposed to electrical fields. They showed that significant strain rates may be commanded through a variation in electrical potential across the gel. Doi and coworkers [2] continued the work into electrochemical artificial muscles as they examined the performance of ionic polymer gels. Although similar, their work demonstrated slightly better actuation characteristics. At about the same time, the groups of Segalman [3], Osada [4] and Pei [5] demonstrated yet more viable configurations of artificial polymeric muscles. Following this early work, Shahinpoor and Mohsen [6] further investigated electro-actuated polymers. As was the case with most configurations of electrochemical artificial muscles, he showed response periods greater than five seconds.

Because the response times of electrochemical artificial muscles are very low and often the chemicals used are not biologically compatible, several investigators have explored other methods of emulating muscle tissues. One approach involves the use of shape-memory alloy (SMA) elements which provide extremely large forces at strains from 2 to 3% cyclically with very little evidence of actuation fatigue. Among the uses are robotic manipulators, appendages and end effectors [7, 8]. Because SMA elements are easily actuated and provide responses under 200 ms, they are fairly suitable as artificial muscles. However, several problems must be solved before they may be successfully used as *in situ* prosthetic devices or implants. One of the more significant difficulties is that the actuation strength of SMA is so high that biological tissues often yield when they encounter such high forces. Other problems include locally high temperatures which can easily cauterize local tissues if the transformation temperatures are too high and the elements are poorly insulated. If animal muscle tissue is to be emulated, then (1) the actuation strains need to be increased from 2 to 3% cyclically to 10 to 20%; (2) the thermal loads imposed on the body must be minimized globally and the temperature must be kept below 120 °F locally; (3) all constituents must be biologically compatible; and (4) response times should be less than 500 ms. This paper will present one new type of super-active material which meets most of these criteria and, accordingly, may be a new type of feasible artificial muscle tissue.

2. Actuator modeling

2.1. Laminate configuration

The super-active shape-memory alloy composite (SASMAC) laminate is composed of two major constituents.

0964-1726/96/030255+06$19.50

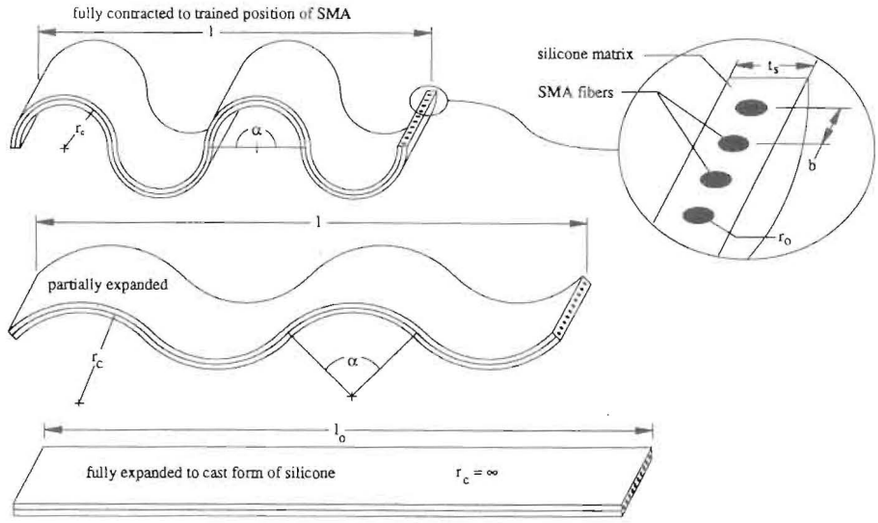

Figure 1. Schematic of hybrid bending-extension SASMAC actuator element.

The first is a series of SMA filaments which are actuated in bending. The second constituent is a very-low-modulus silicone matrix. The low-modulus matrix should be from 20 to 40 Durometer and should be matched to (1) provide fiber stability; (2) insulate the fibers electrically and thermally; and (3) allow for relatively unimpeded motions during maximum deflection. There have been many different types of SASMAC actuators conceived. In general, there are five main types that have been researched: extension-active, shear-active, twist-active, bending-active and hybrid extension.

Generally, the extension-active elements have SMA filaments that are trained only for extension and contraction along the axis of the filament. Because low-modulus, high-strain actuators are needed for artificial muscles, this high-actuation strength, low-strain actuator will not be considered. The second type of SASMAC actuator element is shear-active. This type of element generates in-plane shear forces which may be used to move components. Again, this type of actuator generally induces strains that are much too low to be useful as artificial muscles. The third type of element uses a pair of shear-active elements or a single twist-active element to induce twist deflections. Although several smaller muscle groups provide torsional control and stability, most biological structures do work through axial motions. The fourth type of SASMAC actuator element uses a pair of extension-active or a single bending-active SMA element to induce bending deflections. Although these types of active composites may be highly useful for robotics applications, there are few muscle groups that are capable of actively bending (the tongue is one significant exception). The last form of SASMAC composite uses bending motions to form a type of wavy surface which is capable of extending and contracting. This type of configuration is analogous to the way that active polymers or myosin contract and expand on a molecular level. Figure 1 shows a schematic of a hybrid extension SASMAC composite.

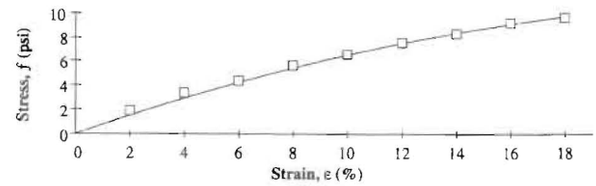

Figure 2. Stress–strain data on low-hardness silicone rubber.

There are two main ways that a hybrid bending-extension SASMAC actuator element may be constructed and energized. The first method uses straight-trained SMA elements which are wound around a curvilinear mandrel and cast with a wavy form. This type of SASMAC element would act as a compression actuator when heated. The major difficulty with this type of active composite is its propensity to buckle even further out-of-plane when exposed to compressive loads. A better form of SASMAC actuator uses bending-trained SMA filaments which are cast into a flat sheet of silicone matrix. When actuated, the SASMAC would contract to a shape akin to that of the trained shape of the filaments. This scheme more closely emulates natural actuator fibers, is not susceptible to buckling, and is shown in figure 1.

2.2. Constituent properties

The two main constituents of the SASMAC composite are SMA filaments and a silicone matrix. Since the type of SASMAC under investigation is specifically intended as a cyclical actuator, the type of SMA was chosen for high resistance to actuation fatigue. From reference [9], Tinel alloy K was selected. Because many sets of muscles undergo millions of cycles in a year (skeletal muscles: 50 000 to 1 000 000/year, pulmonary: 2 000 000 to 20 000 000/year, cardiac: 10 000 000 to 50 000 000/year),

absolutely no actuation fatigue must be present in the system. Accordingly, one way of ensuring that the SMA will experience no fatigue is to expose it to less than 1% strain. Unfortunately, this low strain level does not take full advantage of the capabilities of SMA, but the resistance to fatigue is paramount. This low strain level, however, does significantly simplify the analysis as the SMA remains primarily in the linear range. The modulus of Tinel alloy K at 70 °F is approximately 1.45 Msi, and 8.70 Msi at 320 °F [9].

Because the operational temperatures of the SMA will vary from approximately 100 to 300 °F, a temperature-insensitive, low hardness material was sought. Because silicone rubber met these criteria and was also biologically inert, it was chosen as a suitable matrix material. A special type of 25 Durometer silicone rubber with adhesive agents was tested. A test on a 2" long, 0.1" square coupon yielded the data shown in figure 2.

2.3. Moment and force matching models

Using the geometry of figure 1, it may be assumed that the moments generated by the silicone matrix are matched by the SMA moments at all points, including the apexes. Because the SMA modulus, E_{SMA}, is a function of temperature, the moments generated by the SMA filaments will change. For the low-strain region of interest, it can be seen that the modulus of Tinel alloy K can be approximated as: $E \simeq -0.508 + 0.0288T$, where E (Msi) and T (°F), and $70\,°\mathrm{F} < T < 320\,°\mathrm{F}$. Assuming the stiffness of the silicone matrix may be characterized by a second-order relationship, and assuming the curvature remains constant from section to section, an expression equating these moments may be obtained. If the local strains within the silicone are kept under 2%, then a second-order expression for stress as a function of strain will hold, where E_{s1} is the linear modulus, and E_{s2} characterizes the non-linear effects.

$$\sigma = E_{S1}\varepsilon + E_{S2}\varepsilon^2 \tag{1}$$

Equation (1) is assumed to hold for one-way, tensile strain, with a mirror of the expression valid for compression (for $\varepsilon < 2\%$). If it is assumed that the middle of the laminate (where the SMA filaments are embedded) does only a small amount of work when bent, then an additional bending stiffness due to the presence of silicone (instead of a void from the SMA), will contribute negligibly. Accordingly, a very simple expression for the maximum moment generated by the laminate may be obtained by integrating through the thickness from the middle for each filament segment:

$$M = 2b\int_0^{t_s/2}\left(E_{s1}\varepsilon + E_{s2}\varepsilon^2\right)y\,\mathrm{d}y \tag{2}$$

Because the silicone is cast flat, then actively bent by the curvilinear-trained SMA filaments, a simple relationship may be obtained for the longitudinal strain as a function of depth within the laminate, where y is the through-thickness dimension and is measured from the mid-plane

$$\varepsilon = y/r_c. \tag{3}$$

Using equations (2) and (3), an expression for the moment generated by the silicone is obtained:

$$M_{silicone} = \frac{E_{S1}t_s^3 b}{12r_c} + \frac{E_{S2}t_s^4 b}{32r_c^2} \tag{4}$$

A similar analysis of the SMA filaments is formulated assuming that the filaments have circular cross-sections and trained to a curvilinear state with a zero-stress radius of r_{cmin}. Accordingly, the silicone moment of equation (4) is seen to be balanced by the SMA moment of equation (5):

$$M_{SMA} = \frac{E_{SMA}r_o^4}{4}\left(\frac{1}{r_{c_{\min}}} - \frac{1}{r_c}\right) = \frac{E_{S1}t_s^3 b}{12r_c} + \frac{E_{S2}t_s^4 b}{32r_c^2} = M_{silicone}. \tag{5}$$

Although this rudimentary model neglects many highly non-linear effects which are present in the laminate, it offers a simple and effective method of solution for the local section curvature, r_c. Once the curvature is obtained, it may be cast in terms of the global laminate strain by equation (6).

$$\varepsilon = \frac{2r_c}{l_o}\sin\left(\frac{l_o}{2r_c}\right) - 1. \tag{6}$$

Using the geometry of figure 1 and the basic relationships above, the axial force of the laminate may also be determined and used in an equilibrium relationship. It can be seen that the moments which are balanced in equation (5) may act through a distance to the global laminate mid-plane, as given by equation (7):

$$D = r_c\left(1 - \cos\left(l_o/2r_c\right)\right) = r_c(1 - \cos(\alpha/2)). \tag{7}$$

This force estimation assumes that the external force, F_{ext}, of figure 1 is acting upon the laminate and that it is distributed equally among all the fibers with no applied moment at the end. Equation (8) shows the approximate amount of axial force which is delivered by the SMA filaments.

$$F_{SMA} + F_{matrix} = \frac{E_{SMA}r_o^4}{4(1 - \cos(l_o/2r_c))}\left(\frac{1}{r_{c_{\min}}} - \frac{1}{r_c}\right) - \frac{1}{(1 - \cos(l_o/2r_c))}\left(\frac{E_{S1}t_s^3 b}{12r_c} + \frac{E_{S2}t_s^4 b}{32r_c^2}\right) = F_{external}. \tag{8}$$

The models of equations (5) and (8) are used to optimize free laminate performance. A moment matching plot may be obtained for a SASMAC laminate composed of the silicone described in figure 2 and 10 mil diameter Tinel alloy K. It can be seen in figure 3 that the total laminate strain varies from 0 (totally elongated) to more than 25% (compressed).

Using the moment matching data, the geometric parameters which yield the greatest free- strains may be determined. Figure 4 shows that a spacing ratio of 1 yields an optimum solution at a thickness ratio of $t_s/(2r_o)$ 29. (Further non-dimensionalization is difficult as the constituent behavior is non-linear). It can also be seen that a spacing ratio less than 1 would yield an even stronger optimum. This is physically possible, but would require an offset spacing in the matrix.

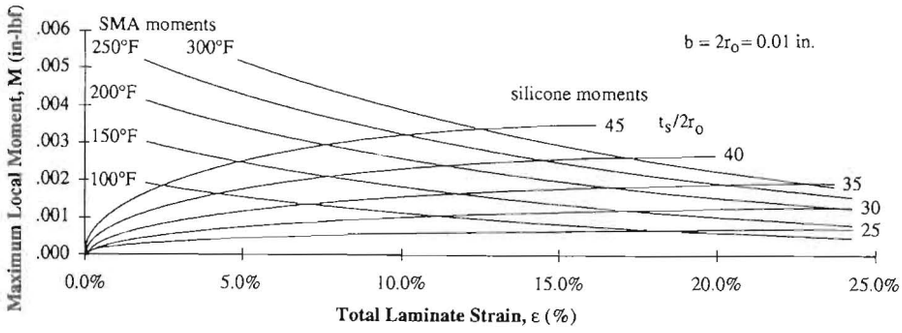

Figure 3. Moment plot for a laminate with curvilinear-trained, straight-cast filaments.

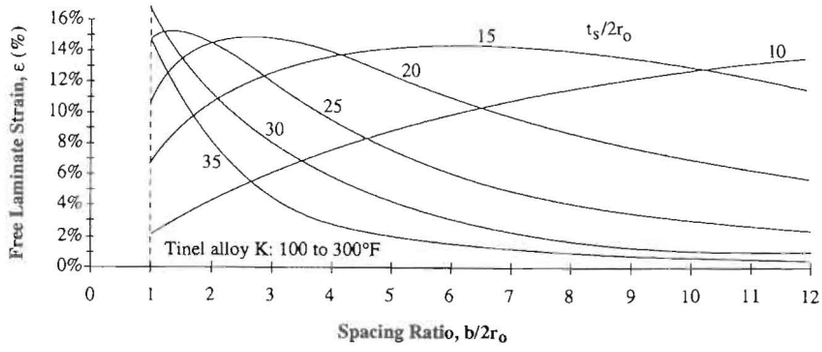

Figure 4. Free laminate strain variation with temperature, spacing ratio and thickness ratio.

3. Actuator construction and testing

3.1. SASMAC actuator configuration and construction

Because the vast majority of muscles in animals operate in pairs, a simple rig with a pair of SASMAC actuators was fabricated in a pull–pull arrangement. The two actuators were clamped rigidly at either end and not allowed to rotate. Both elements were prestrained to 10% less than their cast shape. This imparted a curvilinearity angle of 90° to the laminate. The configuration of the pull–pull SASMAC test rig is shown in figure 5.

Construction was performed in three major stages. First, the SMA filaments were jigged, laid out with tight spacing and fitted with electrical leads on both ends and in the middle. Second, the silicone matrix cast straight around the jigged filaments. Third, the SMA filaments were trained to a minimum radius of 0.5 inches.

Jigging was accomplished by using pressure-sensitive Teflon tape as a backing material with aluminum and brass end clamps. The clamps were mechanically crimped on to the filaments to ensure proper electrical connection. Spaces between the crimped sections were filled with Master Bond conducting epoxy to ensure good electrical connection. Additionally, a pair of 1 mil diameter thermocouples were bonded to the wires with cyanoacrylate to measure filament temperature.

Silicone resin was applied to the free-side of the tape-jigged filaments. A porous backing material of Teflon peel ply was used to facilitate the room-temperature air-cure. After curing at room temperature for two days, the specimen was removed from the mold and the other side was cast, again using the Teflon peel ply. Following the cure cycle, the electrical connectivity of each filament was verified by measuring the individual conductivities of the 10 wires. At the ends of each element, 12 gage multi-strand high-amperage wires were attached.

The SASMAC was then placed in a training jig and the Tinel alloy K filaments were heated and trained to the 0.5" radius curves shown in figure 1. During training, no evidence of matrix failure was detected.

3.2. SASMAC testing

The testing was conducted in plain air with a pair of power supplies connected to each element. The temperature of the expansion side element was maintained at 100 °F (±4 °F). The contraction side was energized to generate temperatures from 120 to 300 °F. After one side had been heated to full temperature, the cycle was reversed and the position of the centerline was recorded. Figure 6 shows the averaged results of the first 20 cycles.

The techniques of section 2 were used to estimate the amount of force present in each section of the laminate. Equation (3) was used to balance the forces of the two parts of the laminate. As can be seen, the predictions of figure 6 are up to 15% higher than the experimental data. In addition to the inaccuracies of the rudimentary model presented earlier, the restraint of the SASMAC ends

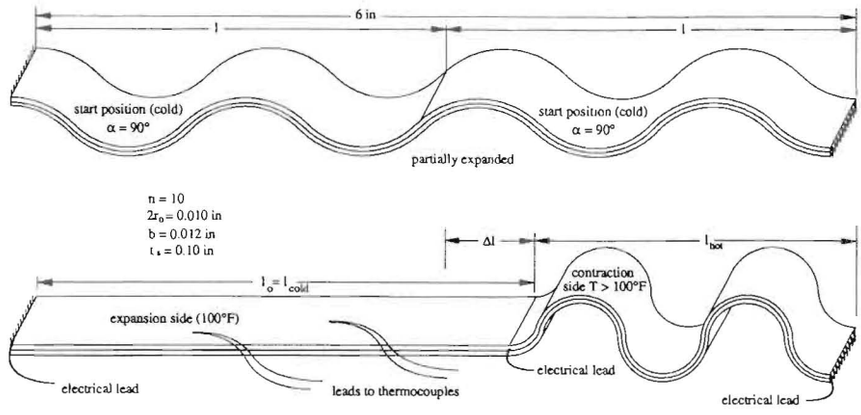

Figure 5. Arrangement of pull–pull SASMAC test rig.

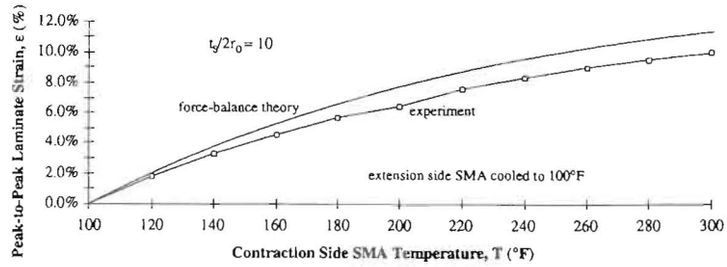

Figure 6. Peak-to-peak laminate strain as a function of contraction side temperature.

adversely affected laminate performance. Still, however, the simplicity and ease of use of the moment and force balance models allow the structural designer to rapidly obtain a performance estimate with reasonable accuracy.

In addition to static testing, a fatigue test was conducted on the pull–pull test specimen. Data were taken for more than 1 000 maximum deflection cycles. As the number of cycles grew, an *increase* in deflection from 2 to 3% was recorded. It is believed that, instead of the SMA being degraded by fatigue, the silicone matrix near the ends started to fail, which allowed less restrained end rotations.

4. Conclusions

This study has shown that a simple moment and force balance is adequate for capturing the fundamental actuation and deflection characteristics of a hybrid SASMAC actuator. This study has demonstrated that a 0.10 inch thick, hybrid SASMAC laminate with 10 mm Tinel alloy K filaments arranged as a pull–pull actuator may generate active strains that are more than 10% of the individual element length. Fatigue testing of the device showed a 2 to 3% deflection increase as the number of cycles approached 1 000.

Acknowledgments

The authors would like to acknowledge the Auburn University Research Grant-in-Aid Program and the Auburn University College of Engineering for supporting this research.

Nomenclature

E	modulus [lb/in^2]
$E\Lambda_{\max}$	actuation strength of adaptive element or material [lb/in^2]
E_{S_1}	first coefficient of silicone stiffness approximation [lb/in^2]
E_{S_2}	second coefficient of silicone stiffness approximation [lb/in^2]
F	force [lb]
l_o	cast length of laminate [in]
r_c	radius of laminate curvature [in]
r_{cmin}	minimum or trained radius of laminate curvature [in]
r_o	radius of SMA filament [in]
t_s	thickness of silicone matrix [in]
α	curvilinearity angle [rad]
ε	laminate strain —
Λ	free actuator element strain —
Subscripts	
ext	externally applied
matrix	silicone matrix
s	silicone or substrate
SASMAC	Super-active shape memory alloy composite
SMA	shape-memory alloy

References

[1] Shiga T and Kurauchi T 1990 Deformation of polyelectrolyte gels under the influence of electric field *J. Appl. Poly. Sci.* **39** 2305–20

[2] Doi M, Matsumoto M and Hirose Y 1992 Deformations of ionic polymer gels by electric fields *Macromol. J.* **29** 5504–11

[3] Segalman D, Witkowski W, Adolf D and Shanipoor M 1992 Theory and applications of electrically controlled polymeric gels *Smart Mater. Struct.* **1** 95–100

[4] Osada Y, Okuzaki H and Hori H 1992 A polymer gel with electrically driven mobility *Nature* **355** 242–424

[5] Pei, Qibing, Inganäa, Olle, Lundström and Ingemar 1993 Bending bilayer strips built from polyaniline for artificial electrochemical muscles *J. Smart Struct. Mater.* **2** 1–6

[6] Shahinpoor and Mohsen 1994 Continuum electromechanics of ionic polymeric gels as artificial muscles for robotic applications *J. Smart Struct. Mater.* **3** 367–72

[7] Swissmetal Advanced Materials and Technologies, Herk-de-Stad, Belgium 1992 *Shape Memory Actuators*

[8] Duerig T W and Melton K N 1989 Designing with the shape memory effect *Materials Research Society International Meeting on Advanced Materials* vol 9, pp 581–97

[9] Raychem Corp. Metals Division, Menlo Park, CA 1989 *Raychem Tinel Shape-Memory Alloys*